Integrative Zoology 2024; 0: 1–18 doi: 10.1111/1749-4877.12829

ORIGINAL ARTICLE

INTEGRATIVE ZOOLOGY

The special adaptation to hypoxia facilitated the expansion of the Asian house rat (*Rattus tanezumi*) into Tibet but not other *Rattus* species

Ruidong CAO,[1,2] Mingyu ZHANG,[1,2] Yi CHEN,[1,2] Guanmei HOU,[1,2] Quansheng LIU,[3] Jianxu ZHANG[1,2] and Yaohua ZHANG[1,2*]

[1]State Key Laboratory of Integrated Management of Pest Insects and Rodents, Institute of Zoology, Chinese Academy of Sciences, Beijing, China, [2]CAS Center for Excellence in Biotic Interactions, University of Chinese Academy of Sciences, Beijing, China and [3]Guangdong Key Laboratory of Animal Conservation and Resource Utilization, Guangdong Public Laboratory of Wild Animal Conservation and Utilization, Institute of Zoology, Guangdong Academy of Sciences, Guangzhou, China

Abstract

Rattus species are thought to live only at altitudes less than 2500 m, but the Asian house rat (*R. tanezumi*) (RT) has recently expanded to altitudes greater than 3500 m in China. Other *Rattus* species, especially brown rats (*R. norvegicus*) (RN), still reach only low altitudes on the Tibetan Plateau. Comparative genomics revealed the positive selection of hypoxia-inducible transcription factors 1 and 2 (HIFs) in RT, with the rapid evolution of HIF pathway genes in RT and *Mus musculus* (MM) but not RN or *R. rattus*. Population genomics revealed that genes associated with energy metabolism and oxygen transport were positively selected in RT compared with the other four *Rattus* species, and two specific substitutions (arginine 31 serine and leucine 33 methionine) were identified in the hemoglobin subunit beta (HBB) in RT. The above results suggested that RT possesses unique genetic adaptations to hypoxia, which was further confirmed by behavioral experiments on RT and RN. Normobaric hypoxia significantly reduced locomotion in RN but not in RT. Moreover, through intraspecific transcriptome analysis, the expression of *Hbb* and genes related to angiogenesis, oxygen transport, and glycolysis was upregulated, and the expression of genes associated with immunological functions in the liver, lungs, and/or sperm was downregulated in RT compared to those in RN. Interspecific transcriptome analysis further revealed that HIF-1α plays a role in modulating the hypoxic adaptation of RT rather than RN. Our work provides genomic, behavioral, and physiological insights into why RT, but not other *Rattus* species, could invade the Tibetan Plateau.

Key words: genomic signature, hypoxia, physiological plasticity, *Rattus tanezumi*, transcriptome

INTRODUCTION

One of the important factors leading to the invasion and geographical redistribution of global mammal species from low altitudes to high altitudes is global warming (Chen *et al.* 2011; Provan & Maggs 2012). However, in high-altitude regions, a decrease in oxygen partial

Correspondence: Yaohua Zhang and Jianxu Zhang, Institute of Zoology, Chinese Academy of Sciences, Beijing, China.
Email: zhangyh@ahu.edu.cn, zhangyh.eco@outlook.com and zhangjx@ioz.ac.cn, zhangjx.rat@outlook.com
*Present address: School of Resources and Environmental Engineering, Anhui University, Hefei, China.

pressure is another main limiting factor for exotic species' survival and reproductive success (Arias-Reyes *et al.* 2021). The genus *Rattus* is one of the largest genera of mammals and includes as many as 66 species. *Rattus* is a late but highly successful invader living on Earth (Wilson & Reeder 2005; Rowe *et al.* 2011). The most important *Rattus* species to humans are three commensal species, namely, the brown rat (*R. norvegicus*, RN), the Asian house rat (*R. tanezumi*, RT), and the black rat (*R. rattus*, RR), which have colonized rural and urban human settlements globally (Kosoy *et al.* 2015). For hundreds of years, these three commensal rat species have undergone extensive global invasions and caused many kinds of harm, especially the transmission of zoonotic diseases such as plague (Kosoy *et al.* 2015). However, even if the *Rattus* rats inhabit locations worldwide and are considered the most successful mammals in the world, they are rarely found at altitudes above 3000 m. This may be related to their poor tolerance to low oxygen levels (Arias-Reyes *et al.* 2021).

Of the three commensal rat species, RT rats are the most recent invaders; RT rats have invaded the South Pacific, the United States, and African countries from Southeast Asia in recent decades (Kosoy *et al.* 2015). In China, RT rats inhabit the Yangtze River valley and southern region; however, in recent decades, this range has greatly expanded to high latitudes and altitudes in regions such as central Hebei Province, the Hexi Corridor in Gansu Province, Xining City in Qinghai Province, and Lhasa City and Shannan City in Tibet (Zhang *et al.* 2000; Guo *et al.* 2019; Liu *et al.* 2021; Jing *et al.* 2022). In Tibet, RT rats have expanded to altitudes above 3500 m, while other *Rattus* species, especially RN rats, are still found mainly on the edge of the Qinghai–Tibet Plateau (Chen *et al.* 2021a).

The RT population in China can be divided into four lineages. The Tibetan lineage was differentiated from the other three lineages at low altitudes and is most closely related to rats located around Chengdu City. This suggests that RT rats might invade the Tibetan Plateau from the Chengdu Plain, probably via the Sichuan–Tibet highway, construction began in 1950, and it originates from the Chengdu Plain, not from the border ports of entry with South Asian countries (Guo *et al.* 2019; Chen *et al.* 2021a). In Tibet, the first recorded distribution of RT rats was on the edge of the Tibetan Plateau. These RT rats were recorded by the 1970s fauna survey in areas such as Qamdo City, Basu County, and Bomê County, which have an average altitude of more than 3000 m (Feng *et al.* 1986). By 2006, RT rats had invaded Nyingchi City, Lhasa City, and Shannan City, becoming the dominant rat species (Li *et al.* 2009a). From the Chengdu Plain to Qamdo City and Lhasa City, the altitude increased to an average of approximately 3500 m, and the oxygen content decreased to 13.5%. There are five *Rattus* species, RT, RN, *R. nitidus* (RNi), *Rattus andamanensis* (RA), and *R. losea* (RL), distributed on the Chengdu Plain; except for RT, the others can be found mainly below an altitude of 2500 m (Feng *et al.* 1986; Wilson & Reeder 2005; Huang *et al.* 2008). Therefore, compared with other *Rattus* species, RT rats may preadapt to hypoxia.

Mammals living in hypoxic plateau environments usually develop unique genetic and physiological adaptations to prevent an imbalance in energy supply and demand; these adaptations include increasing anaerobic metabolic capacity and oxygen transport capacity (Storz *et al.* 2010). For example, yak (*Bos grunniens*) genes related to glycolysis showed positive selection compared with cattle (*B. taurus*) (Qiu *et al.* 2012). In the plateau zokor (*Myospalax baileyi*), genes related to fatty acid beta-oxidation have undergone accelerated evolution compared to those in RN rats, and genes related to vascular development have been positively selected, resulting in adaptation to hypoxia (Shao *et al.* 2015). We recently reported that the RT rat population in Lhasa, Tibet, has an adaptive genetic mutation for low oxygen levels compared with RT rats at low altitudes (Chen *et al.* 2021a). However, this does not fully explain why RT rats rather than other *Rattus* rats invade high-altitude localities. Here, we hypothesized that, compared with other *Rattus* species, RT rats living at low altitudes evolved unique genetic hypoxic adaptations, like *Mus musculus* (MM) adapted to the plateau.

Long-term hypoxia exposure induces different physiological responses, such as increased right ventricular hypertrophy and a decreased alveolar surface area and metabolic rate, in RN rats compared with house mice, explaining that mice can be found at high altitudes while rats are absent at these altitudes (Jochmans-Lemoine *et al.* 2015; Arias-Reyes *et al.* 2021). The adaptive physiological plasticity to hypoxia can be well reflected by changes in gene expression patterns in the liver and lung through transcriptomic analysis (Baze *et al.* 2010; Ge *et al.* 2021). The potential for male fertility can be predicted through sperm transcriptome assessment; thus, the effects of hypoxia on the function of sperm in spermatogenesis, fertilization, and embryo development can be validated by gene expression (Indriastuti *et al.* 2022). We hypothesized that RT rats would have a greater physiological tolerance to hypoxia than would RN rats, a typical relative species not adapted to low oxygen,

and such results could be illustrated by transcriptomic analysis of the lung, liver, and sperm.

MATERIALS AND METHODS

Ethics statement

All animal work was performed according to the Institutional Guidelines for Animal Use and Care at the Institute of Zoology, Chinese Academy of Sciences, China (no. IOZ13015).

Comparative genome analysis

To investigate the genomic traits underlying the hypoxic adaptability of RT rats, the RT genome was assembled by sequencing in our previous study (Chen *et al.* 2021a). Three rodent genomes (MM, RN and RR) (Table S1, Supporting Information) obtained from NCBI were used to perform comparative genome analysis. We used OrthoFinder v2.2.7 (Emms & Kelly 2019) to identify candidate single-copy orthologs and construct the phylogenetic tree. We used Muscle v1.2.4 (Edgar 2004) to align the amino acid sequences of all single-copy genes and then used the pal2nal.pl script from the PhaME toolkit (Shakya *et al.* 2020) to convert the sequences to codon alignments. We used the Codeml program in Paml v4.9 (Yang 2007) to identify positively significant genes (PSGs) and rapidly evolving genes (REGs). Briefly, the branch-site model (model = 2, NSsites = 2) was used to indicate PSGs, and the branch model (one-ratio [M0] model, two-ratio [M2] model, and NSsite = 0) was used to indicate REGs. Each species in the phylogenetic tree were designated respectively as the foreground branch. Likelihood ratio tests were used to calculate the values. False discovery rate (FDR) correction was used to control for multiple comparisons. PSGs and REGs (P-adjust < 0.05) were identified, and GO enrichment analyses were performed via Metascape (Zhou *et al.* 2019).

Sample collection and whole-genome resequencing

Thirty-three rats from five *Rattus* species were analyzed by a population genomic framework (Table S2, Supporting Information). Six RT rats, ten RN rats, and seven RNi rats were obtained from previous studies (Teng *et al.* 2017; Chen *et al.* 2021a; Chen *et al.* 2021b). Five RL rats and RA rats were trapped on the outskirts of Guangzhou City, Guangdong Province, and identified by morphological characteristics and mitochondrial cytochrome oxidase subunit I as barcodes (Table S3, Supporting Information). DNA extraction, library preparation, and sequencing with 2 × 150 bp on the Illumina HiSeq X Ten instrument were performed at Novogene Bioinformatics Technology Co., Ltd. (Tianjin, China). After filtering out the raw sequencing reads containing adapters and reads of low quality, the remaining clean reads were mapped to the reference genome of the RN, RGSC5.0, using BWA v0.7.12 with default parameters (Li & Durbin 2009). SAMtools v1.2 (Li *et al.* 2009b) was used to sort the reads, and the MarkDuplicates tool in Picard v1.13 (http://broadinstitute.github.io/picard/) was used to remove PCR duplicates. Reads mapped to two or more locations were filtered out.

Single-nucleotide polymorphism calling and filtering

The Genome Analysis Toolkit (GATK v3.7) HaplotypeCaller protocol (McKenna *et al.* 2010) was used for SNP calling. SNPs were further filtered by applying the following criteria: QD < 10.0, DP < 4.0, FS > 10.0, QUAL < 30.0, ReadPosRankSum < − 8.0. Additionally, the sites with a minor allele frequency < 0.05 or that included more than 10% missing genotypes were filtered out. The filtered high-quality SNPs were subsequently retained for analysis.

Phylogenetic analysis, principal component analysis, genetic diversity, and LD analysis

Snphylo (Lee *et al.* 2014) was used to construct a maximum likelihood (ML) tree with the parameter "- l 0.1" GCTA (Yang *et al.* 2011) was conducted for principal component analysis (PCA) with the parameters "–independent-pairwise 50 5 0.05." VCFtools v0.1.16 (Danecek *et al.* 2011) was used to measure pairwise nucleotide diversity with a 100-kb sliding window. Five individuals of each rat species were used to estimate pairwise linkage disequilibrium (LD) via PopLDdecay v3.41 (Zhang *et al.* 2019).

Detection of selective sweeps

To identify the genetic traits related to hypoxic adaptation in RT rats compared with those in other *Rattus* species, we identified selective sweeps in the RT genome via pairwise comparisons between RT versus RN, RL, RA, and RNi, respectively. First, we performed a genome

scan using an updated cross-population composite likelihood approach ratio (XP-CLR) (Chen *et al.* 2010). This approach has greater power than other approaches for detecting selective sweeps via the likelihood method of multilocus allele frequency differentiation and could be used in closely related species analysis. This is because it is less biased by demographic history and uncertainty in recombination rates and does not maintain strict window boundaries (Pendleton *et al.* 2018). Since we are searching for regions under selection in the RT genome, other *Rattus* species were set up as our reference population, respectively. A 0.05-cm sliding window with 2000 bp steps across the whole genome was used for scanning, and the number of SNPs assayed in each window was set to 250. The mean likelihood scores in 100-kb sliding windows with a step size of 20 kb across the genome were calculated. The regions with the highest XP-CLRs, accounting for 1% of the windows, were considered the selected regions. Then, we performed cross-population extended haplotype homozygosity (XP-EHH), which is also used in closely related species analysis, with a window size of 100 kb and a step size of 20 kb. Selection can be performed when the haplotype under selection is near fixation in one population or polymorphic in the other population by comparing the lengths of haplotypes between populations and using the selscan program (Szpiech & Hernandez 2014). The *P* value of each SNP was estimated using the normal distribution of standardized XP-EHH values. The significant SNPs ($P < 0.01$) with a distance of < 100 kb were clustered as candidate regions for further analysis. Generally, a positive XP-EHH value suggests selection in the target population, while a negative XP-EHH value indicates selection in the reference population (Sabeti *et al.* 2007). The RT rats were set as the target population, and the other *Rattus* species were set as the reference population. We selected positive XP-EHH values. Finally, we estimated the genome-wide distribution of the fixation index (Weir and Cockerham's F_{ST}) between RT rats versus other *Rattus* species using vcftools v0.1.16 (Danecek *et al.* 2011) with a window size of 100 kb and a step size of 20 kb. Like in most interspecific comparisons, the F_{ST} values of the four groups were highly differentiated according to our calculations (Blackwell *et al.* 2021). We did not select regions with the highest F_{ST} values to avoid losing important information. The overlapping regions detected by XP-CLR and XP-EHH were determined to be candidate regions under positive selection, and the F_{ST} values were mapped. The genes contained in the selected sweep regions were candidate PSGs. We performed an enrichment analysis of the PSGs via the online tool Metascape and clusterProfiler 4.0 (Wu *et al*. 2021). The identified mutations in the PSGs were predicted by PolyPhen-2 (Adzhubei *et al.* 2013).

Animals used in the experiments

Wild RN rats and RT rats were captured from Beijing and Shanxi Province (China), respectively. All the rats were maintained as an outbred colony of 300–400 rats in our laboratory. All animals were kept in plastic rat cages (37 × 26 ×17 cm) in two separate rooms (14:10 h light: dark photoperiod, lights on at 17:00) and were maintained at 22 ± 2°C. Food (standard rat chow) and water were provided *ad libitum*.

Hypoxic and control chambers

The chambers were made of plastic boxes (60 × 42 × 31 cm) with sealed lids and air/nitrogen pipe outlets/inlets. Pure N_2 and air were piped into the hypoxic/control chambers. The concentrations of O_2 and CO_2 were continuously monitored using O_2 and CO_2 meters, and the flow rates were adjusted using flowmeters. In the hypoxic chambers, the O_2 concentration was maintained at 13.5% ± 0.5% (equivalent to the O_2 concentration at an altitude of 3500 m). In the control chambers, the O_2 concentration was 20%. All the chambers kept a CO_2 concentration of 0.04% ± 0.01% and were under normobaric conditions.

Testing behavior in normobaric hypoxia

The behavioral changes in the RT and RN rats in a hypoxic environment were examined through behavioral experiments. Twenty-four adult male RN rats and RT rats were used. Half of these rats were assigned to the hypoxic group, and the other half were assigned to the control group. The RN and RT rats of the hypoxic group were assigned in pairs and simultaneously into a single chamber. Each trial lasted for an hour. The time spent on locomotion (moving the limbs) and resting (lying on one's stomach) by the subjects was recorded by stopwatches. The same procedures were performed for the control group. The negligible impact of pairing behavior can be attributed to the frequent coexistence of RT and RN rats in their natural habitat without conflicts.

Treatment under normobaric hypoxia

Eight adult male RN rats and RT rats were used, half of which were used as the hypoxic group (rats in the hypoxic chambers), and the other half were used as the

control group (rats in the control chambers). Each rat was weighed and then placed in a hypoxic or control chamber for 5 days. There was no significant difference in body weight between the hypoxic and control groups before hypoxia exposure (RN: 208.2 ± 13.86 g vs. 205.9 ± 12.48 g, $t = 0.122$, $P = 0.907$; RT: 130.5 ± 5.45 g vs. 130.3 ± 6.16 g, $t = -0.024$, $P = 0.981$, $n = 4$). On the morning of the sixth day, each rat was weighed again and immediately decapitated. The liver, lung, and sperm were immediately dissected, rapidly frozen in liquid nitrogen, and stored at −80°C until use. The liver, lung, and sperm were used for transcriptome analysis.

RNA sequencing and intraspecific transcriptome analysis

RNA contraction, library preparation, and sequencing were performed at Novogene Bioinformatics Technology Co., Ltd. (Tianjin, China). Clean reads were obtained by removing adapter-containing reads, poly-N-containing reads, and low-quality reads from the raw data, followed by mapping to the reference RN rat genome mRatBN7.2 using Hisat v2.2.1 (Kim *et al.* 2015). Gene counts were performed using StringTie v2.1.4 (Pertea *et al.* 2015). DESeq2 v1.36 (Love *et al.* 2014) was used to determine differentially expressed genes (DEGs). The genes that exhibited a $|\log_2(\text{fold change})| \geq 1$ and a FDR adjusted $P < 0.05$ were considered DEGs. Functional enrichment analysis was performed for the upregulated and downregulated DEGs via the Metascape. Terms were grouped into clusters based on their membership similarities with the option of $P < 0.01$, a minimum count of 3, and an enrichment factor > 1.5. The most statistically significant term within a cluster was chosen to represent the cluster.

Interspecific transcriptome analysis

The clean reads of the two species were mapped to their genomes using Hisat v2.2.1. Counts of each gene were calculated with StringTie v2.1.4. 1:1 orthologous gene was generated using the reciprocal BLAST module from TBtools v1.098769 (Chen *et al.* 2020). Then, a 1:1 orthologous gene count was used to perform differential expression analysis between the RN rats and the RT liver, lung, and sperm with DESeq2 v1.36. Orthologous gene lengths could vary between RT and RN rats. Thus, we calculated the length matrix of these genes with the R package rtracklayer v1.56.1 and input these genes into the DESeq2 "DESeqDataSet" object for downstream normalization. RT/RN was set as the parameter for "treat/control" in the pipeline of DEG analysis. The genes that exhibited $|\log_2(\text{fold change})| \geq 1$ and FDR-adjusted $P < 0.05$ were considered DEGs; those with $\log_2(\text{fold change}) \geq 1$ were considered highly expressed genes in RT. Those with ≤ -1 were considered highly expressed genes in RN. The enrichment analysis pipeline of the DEGs was consistent with that described above.

qRT-PCR analysis

Reverse transcription was performed using HIFIScript gDNA Removal RT MasterMix (Perfect Real Time) (CWBIO Bio, Inc., Beijing, China). The resulting cDNA was amplified using an Mx3005P quantitative PCR system (Stratagene, La Jolla, CA, USA), and the relative abundance of the mRNAs of the target genes was determined using a MagicSYBR mixture (CWBIO Bio, Inc., Beijing, China) according to the manufacturer's instructions. The sequences of PCR primers used are listed in Table S3, Supporting Information. The housekeeping gene *Actb* (*β*-Actin) was used as a control to normalize the relative mRNA levels. The CT values of the verified genes are listed in Table S4, Supporting Information. The relative expression level was calculated by the $2^{-\Delta\Delta Ct}$ method, and the CT value corresponded to the threshold cycle. Significance was tested by an independent sample *t*-test or Wilcoxon signed-rank test. Differences were considered to be statistically significant at $P < 0.05$.

RESULTS

Hypoxia-related genes of RT identified through comparative genomic analysis

We identified 376, 891, 3183, and 419 PSGs and 113, 122, 1776, and 2194 REGs for RN, RR, RT, and MM, respectively (Tables S5–S12, Supporting Information). Some genes related to hypoxic adaptation were enriched exclusively in the PSGs of RT, including "response to hypoxia" and "response to decreased oxygen levels." These genes included *Epas1, Hif-3α, Vegfa, Notch1, Ramp2, Pdgfa*, and *Angpt2* (Fig. 1b). Three unenriched hypoxia-related PSGs, *Mcam, Slc29a1, and Hmox1*, were identified in RT (Fig. 1b).

RT and MM shared eight hypoxia-related REGs (*P*-adjust < 0.05), namely, *Adam9*, *Arnt*, *Egln3*, *Ednrb*, *Pgf*, *Sec24b, Pdgfa*, and *Angpt2* (Fig. 1b). Moreover, RT and MM possess unique REGs adapted to hypoxia (RT: *Slc29a1*; MM: *Spint1, Sirt2*) (Fig. 1b). Neither the RN nor the RR rats had hypoxia-related PSGs, and the MM had no hypoxia-related PSGs.

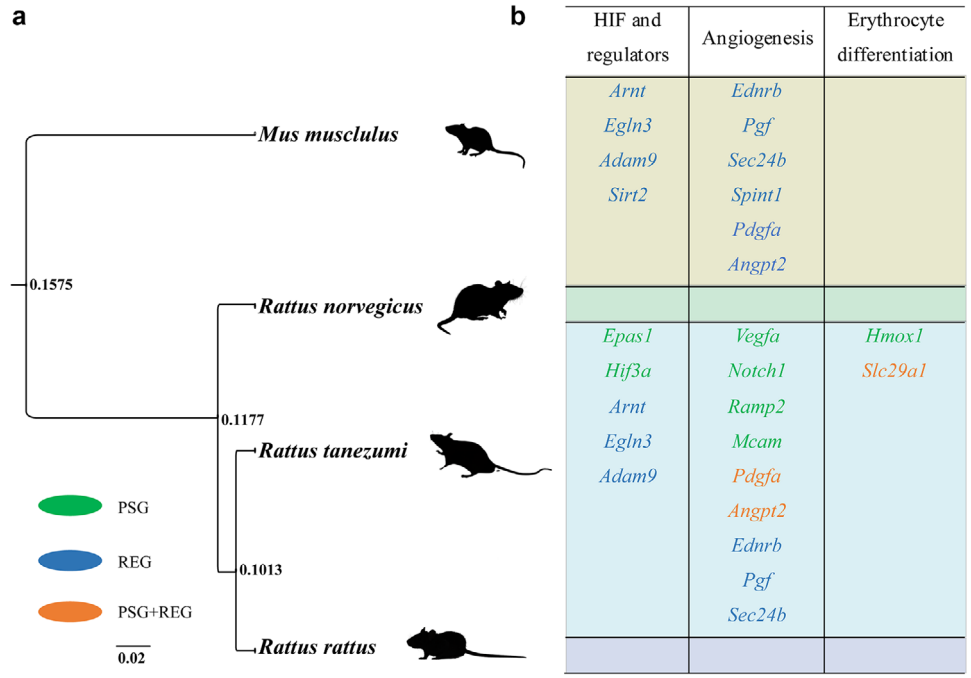

Figure 1 Phylogenetic relationships of four species and positively significant genes (PSGs) and rapidly evolving genes (REGs) associated with hypoxia. (a) The phylogenetic tree of four species was built by OrthoFinder using the default parameters. (b) PSGs and REGs related to hypoxia in the four corresponding species. Green font: PSGs, identified with the Codeml program in Paml v4.9 with the branch-site model (model = 2, NSsites = 2). Blue font: REGs, identified with the branch model (one-ratio (M0) model, two-ratio (M2) model, and NSsite = 0). Orange font: PSG + REG.

Genomic patterns of five *Rattus* species revealed by population genomic analysis

We identified 17 583 703, 6 323 357, 38 565 643, 20 016 714, and 16 062 738 SNPs in the RNi rats, RN rats, RT rats, RL rats and RA rats, respectively. PCA and phylogenetic analysis revealed that RT rats shared the closest genetic relationship with RL rats (Fig. 2a,b). RT rats had the greatest nucleotide diversity, and RN rats had the smallest (Fig. 2c). LD decreased more slowly in RN rats than in the other *Rattus* species (Fig. 2d).

Selective sweeps in the RT Genome compared with those in the other four *Rattus* species

We subsequently identified the PSGs located in outlier regions of the XP-CLR, XP-EHH, and F_{ST} analyses, revealing 397 in the RT versus RA comparison, 371 in the RT versus RNi comparison, 341 in the RT versus RL comparison, and 380 in the RT versus RN comparison (Tables S13–S16, Supporting Information). Twenty-five PSGs were shared among the four groups (RT vs. other *Rattus* species) and were enriched in ethanol oxidation and binding of sperm to the zona pellucida (Fig. S1, Supporting Information). The results of separate enrichment analyses of the four groups of genes revealed 15 shared enrichment terms via Metascape enrichment, including "glycolysis/gluconeogenesis," "pyruvate metabolism," "fatty acid oxidation," "terpenoid metabolic process," and "retinoid metabolic process" (Fig. S2, Supporting Information).

Only in the RT versus RN comparison did we identify a term associated with oxygen transport (oxygen binding), involving the *Hbb*, *Hbb-b1*, *Alb*, and *Ido1* genes (Fig. 3f). We detected two nonsynonymous substitutions in *Hbb* that are unique to RT rats compared to other *Rattus* species. These substitutions led to amino acid changes at positions 31 and 33, with ARG31 replaced by SER31 and Leu33 replaced by Met33 (Fig. 3a–d), and these changes were consistent across all six RT rats that underwent sequencing in this study. The prediction of PolyPhen-2 indicated the significant functional impact of these substitutions (site 31, PolyPhen-2 score = 0.826; site 33, PolyPhen-2 score = 0.940) (Fig. 3e and Fig. S3, Supporting Information).

In the RT versus RN comparison, there were more terms associated with energy metabolism, including

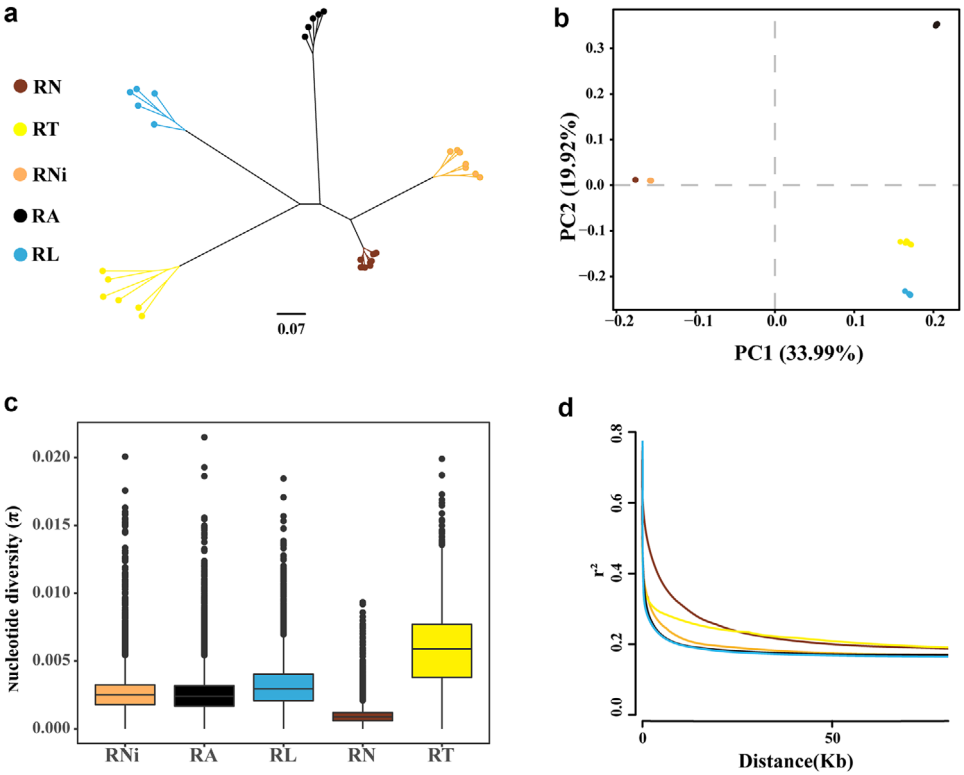

Figure 2 Population genomic analyses of five *Rattus* species. RT, *Rattus tanezumi* (yellow); RL, *R. losea* (blue); RA, *Rattus andamanensis* (black); RNi, *R. nitidus* (orange); and RN, *R. norvegicus* (brown). (a) Maximum likelihood phylogenetic tree based on whole-genome single nucleotide polymorphisms (SNPs). (b) Plots of principal component 1 versus principal component 2 (PC1 vs. PC2) for all rats. (c) Nucleotide diversity for each rat species. (d) Linkage disequilibrium (LD) decay for each rat species. The same numbers of individuals were chosen randomly for each population to calculate r^2.

glycolysis, starch and sucrose metabolism, protein digestion and absorption, and fatty acid degradation (Fig. 3g), than in the other groups. In addition, *Slc39A12, Ank2*, and *Nos1ap* are involved in oxygen transport.

Behavioral performance of RT and RN rats exposed to hypoxia

During hypoxic exposure, the locomotion time decreased ($t = 4.655$, $P < 0.01$, $n = 12$), and the rest time increased in the RN rats ($t = 2.953$, $P < 0.01$, $n = 12$) (Fig. 4a,b). The locomotion time of the RT rats did not change during hypoxia exposure (Fig. 4a). RT rats did not exhibit resting behavior (Fig. 4b).

Hypoxia-induced changes in the transcriptomes of the liver, lung, and sperm in RT and RN

There was no significant difference in body weight change after the experiment between the hypoxic and control groups (RN: 11.71 ± 3.47 g/100 g vs. 7.64 ± 3.87 g/100 g, $t = 0.783$, $P = 0.463$, $n = 4$; RT: 7.03 ± 0.91 g/100 g vs. 2.98 ± 1.48 g/100 g, $t = 2.237$, $P = 0.58$, $n = 4$). Principal component analysis (PCA) revealed that the experimental and control groups tended to separate from each other in the lung along PC1 and liver along PC2 but not in the sperm of RT rats (Figs S4–S6b, Supporting Information). Among the RN rats, the experimental and control groups did not exhibit separation in the lung, liver, or sperm (Figs S4–S6a, Supporting Information). A total of 669 DEGs were identified in the RT rats and 47 DEGs were identified in RN rats between the experimental and control groups (Fig. S7, Supporting Information). In detail, for hepatic DEGs, there were 229 in RT rats (132 upregulated and 97 downregulated) and 11 in RN rats (4 upregulated and 7 downregulated). For pulmonary DEGs, 186 were detected in RT rats (143 upregulated and 43 downregulated) and 30 were detected in RN rats (5 upregulated and 25 downregulated). For the spermic DEGs, there were 254 in RT rats (97 upregulated and 157

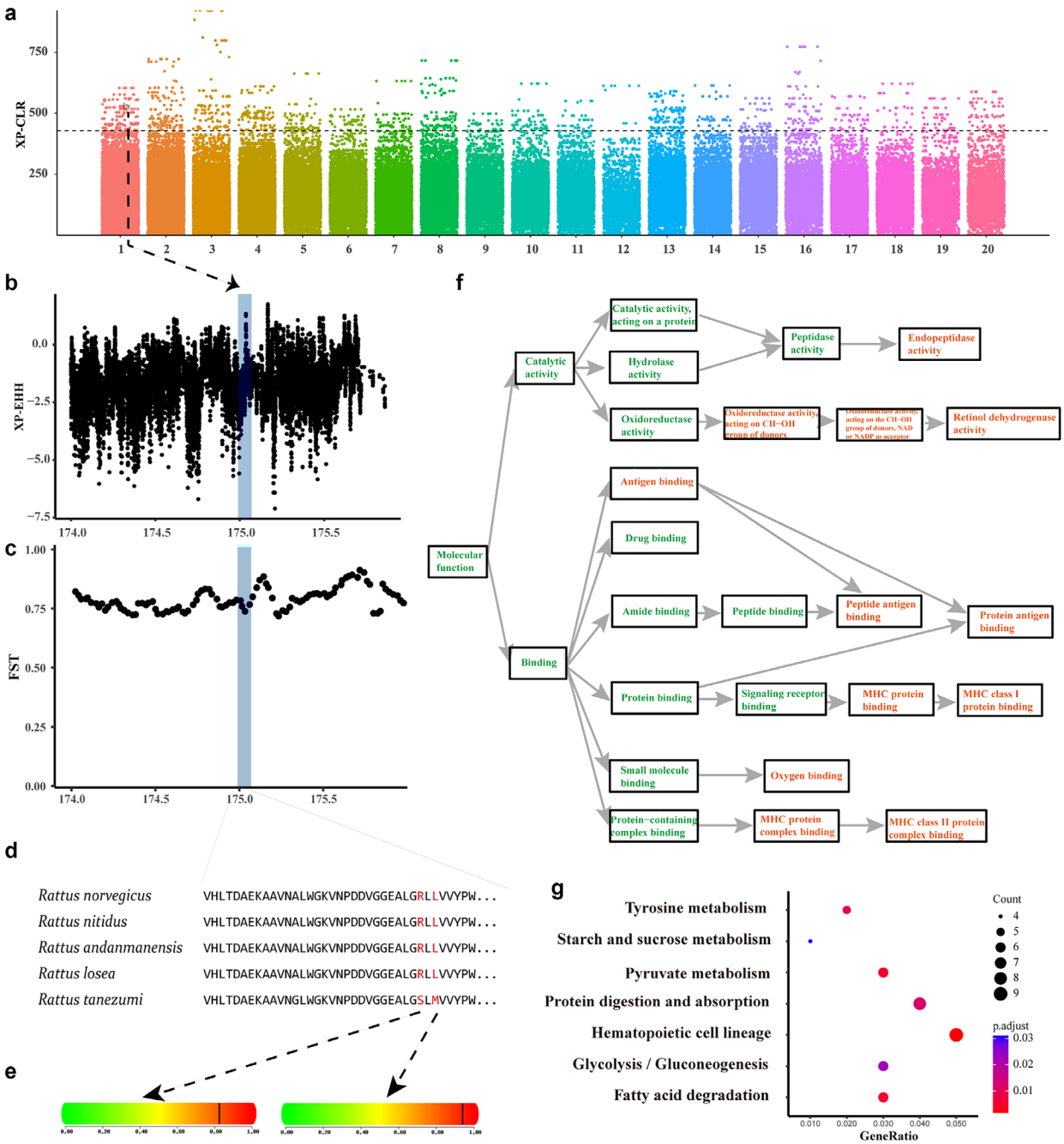

Figure 3 Genomic regions with selective sweep signals in the *Rattus tanezumi* (RT) versus *R. norvegicus* (RN) comparisons. (a) Distribution of the cross-population composite likelihood ratio (XP-CLR) for 100-kb windows with 20-kb steps. The black horizontal line corresponds to the top 1% significance level threshold. (b) Score of standardized cross-population extended haplotype homozygosity (XP-EHH) for each single nucleotide polymorphism (SNP) along chromosome 1. (c) Population differentiation (F_{ST}) between RT and RN rats. The regions shaded in blue in (b) and (c) represent the signals of *Hbb* of XP-EHH and F_{ST} on chromosome 1. (d) Multi-species alignment of two amino acid substitutions (arginine 31 serine and leucine 33 methionine) in hemoglobin subunit beta (HBB). (e) Amino acid substitution scores were predicted using PolyPhen-2 (site 31 = 0.826; site 33 = 0.940). (f) Gene Ontology (GO) enrichment of genes covered in the sweep regions of RT versus RN via clusterProfiler. The orange font indicates significantly enriched categories in the RT. (g) Pathway related hypoxic adaptation in Kyoto Encyclopedia of Genes and Genomes (KEGG) enrichment analysis of genes covered in the sweep regions of RT versus RN via clusterProfiler.

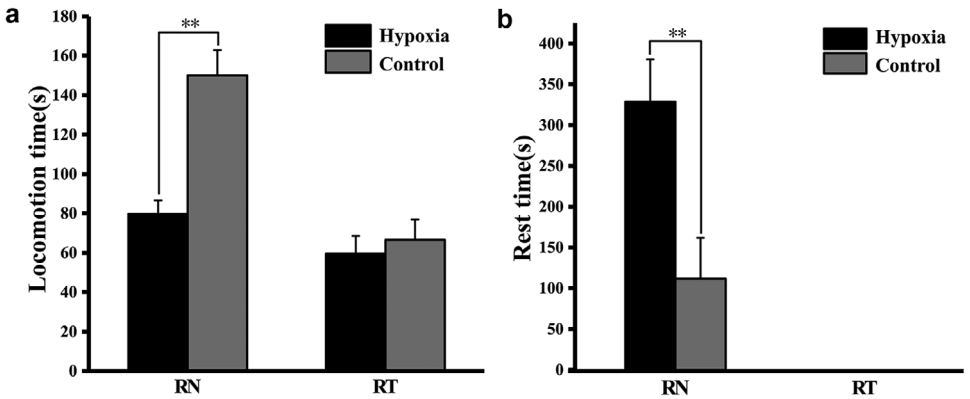

Figure 4 Behavioral performance under hypoxic and normoxic conditions. (a) Total locomotion time. (b) Total rest time ($n = 12$ for each group; mean ± SE; $**P < 0.01$; paired *t*-test or Wilcoxon signed-rank test; RN, *Rattus norvegicus*; RT, *R. tanezumi*).

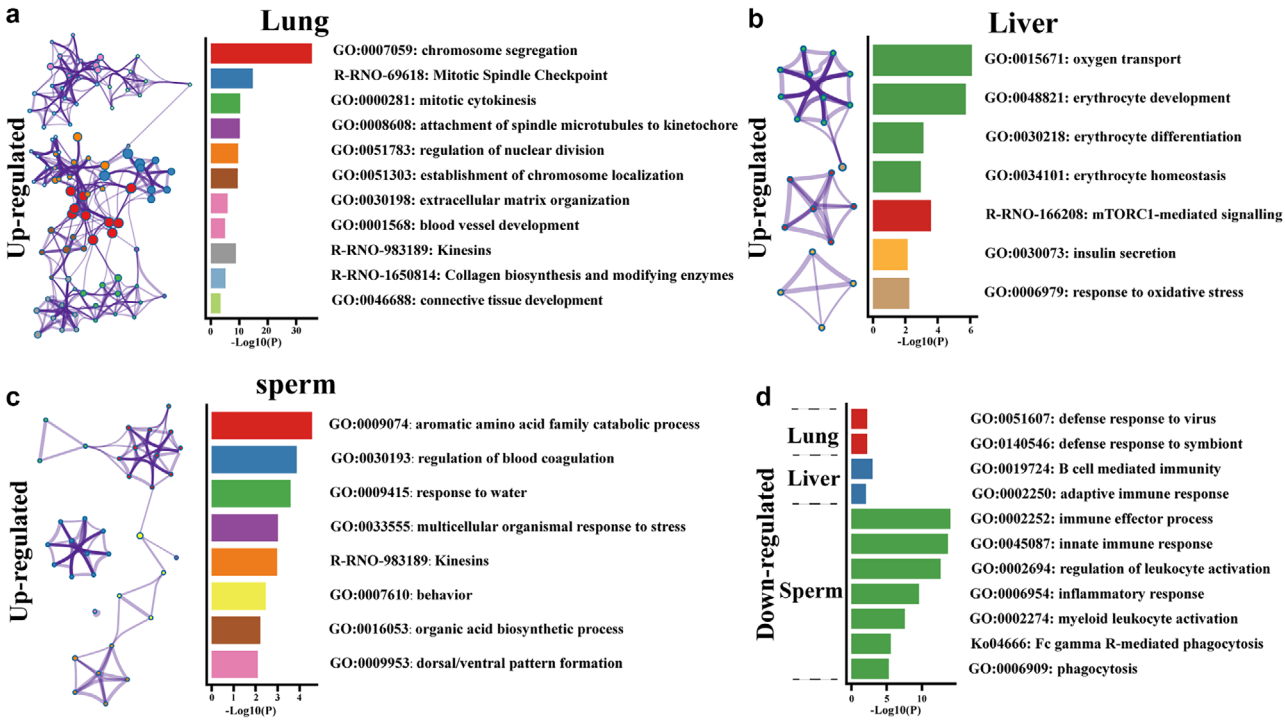

Figure 5 Characterization of differentially expressed genes (DEGs) of *Rattus tanezumi* (RT) rats after hypoxia exposures; $n = 4$. (a) Upregulated genes in the lung of RT. (b) Upregulated genes in the liver of RT. (c) Upregulated genes in the sperm of RT. (d) Downregulated genes in RT. Panels (a)–(c) consist of a network and a bar chart. Network, obtained by Metascape analysis, was a cluster of enriched terms, where each node represents an enriched term, its size is proportional to the number of input genes associated with that term, and its color indicates its cluster identity. Terms were linked by an edge with a similarity score > 0.3. The representative terms from each cluster are displayed on the right.

downregulated) and six in RN rats (2 upregulated and 4 downregulated).

In the lungs, 251 terms were enriched based on the upregulated DEGs in RT rats; these terms were associated mainly with cell division, connective tissue development, blood vessel development, and so on (Fig. 5a). In the liver, 59 terms were enriched according to separate enrichment analyses of the upregulated DEGs in RT rats,

including "oxygen transport," "erythrocyte development," "mTORC1-mediated signaling," "insulin secretion," and "response to oxidative stress" (Fig. 5b). In sperm, 39 terms were enriched through separate enrichment analyses of the upregulated DEGs in RT rats. These genes were involved in the "aromatic amino acid family catabolic process," "organic acid biosynthetic process," "regulation of blood coagulation," "kinesins," "dorsal/ventral pattern formation," and other functions (Fig. 5c). The three groups of downregulated DEGs were enriched primarily in the immune system and included genes related to the "defense response to viruses," "B-cell-mediated immunity," and "regulation of leukocyte activation" (Fig. 5d).

In RN rats, only nine terms ($P < 0.01$) were enriched for the downregulated DEGs in the lung; these genes are involved in "extracellular matrix organization" and "muscle contraction".

Comparison of the interspecific transcriptomes of the lung, liver, and sperm in RT and RN

We evaluated the genes with high expression in the same tissue or cell in these two rat species, namely, 1480/1243 in the lung of RT/RN and 1340/1344 in the liver of RT/RN; 1544/1452 in the sperm of RT/RN under normoxic conditions; and 1733/1276 in the lung of RT/RN and 1441/1326 in the liver of RT/RN and 1495/1542 in the sperm of RT/RN under hypoxic conditions.

Under normoxic conditions, terms in the liver (RT: 82, RN: 115), the lung (RT: 99, RN: 117), and the sperm (RT: 76, RN:161) were involved in various aspects of function (Figs S8–S13, Supporting Information). Under hypoxic conditions, in the lung, 162 terms were primarily associated with cell division and regulation of blood pressure (Fig. S14b, Supporting Information) in RT rats, and 220 terms were related mainly to immune regulation in RN rats. In the liver, 114 terms were mainly associated with a variety of metabolic processes, such as the fatty acid metabolic process (Fig. S14a, Supporting Information) in RT rats, and 112 terms were related to various aspects of functions in RN rats. In the sperm, 65 terms in RT rats and 139 terms in RN rats were related to various aspects of function.

Furthermore, five hypoxia-related genes were expressed at higher levels in RT rats than in RN rats: *Upk1a* (lung: $\log_2$ (fold change) = 5.9, P-adjust = 4.39×10^{-201}; liver: $\log_2$ (fold change) = 14.8, P-adjust = 2.73×10^{-45}), *Gpbar1* (lung: $\log_2$ (fold change) = 9.5, P-adjust = 3.68×10^{-60}; liver: $\log_2$ (fold change) = 13.6, P-adjust = 2.85×10^{-38}), *Ghr1* (lung: $\log_2$ (fold change) = 10.1, P-adjust = 4.45×10^{-18}; liver: $\log_2$ (fold change) = 10.0, P-adjust = 1.5×10^{-4}), *Ftmt* (lung: $\log_2$ (fold change) = 8.0, P-adjust = 5.8×10^{-4}), and *Nox3* (lung: $\log_2$ (fold change) = 7.1, P-adjust = 2.3×10^{-3}) (Fig. S14c,d, Supporting Information).

Validation of qRT–PCR

qRT-PCR confirmed that hepatic *Hbb, Alas2, Tk1, Gucy2c*, and *Hspb1* and pulmonary *Col1a1, Ntrk2, Mgarp, Ccna2*, and *Eln* were upregulated in hypoxia-treated RT rats (Fig. S15, Supporting Information).

DISCUSSION

Based on our comparative genomic analysis, we showed that, compared with RN rats, RR rats, and MM, RT rats had hypoxia-related genes that underwent positive selection and rapidly evolved. This evolution was similar to that of MM but not that of RN or RR rats. Population genomics revealed that the genes associated with energy metabolism and oxygen transport were under positive selection in RT rats compared to those in RN rats, RL rats, RA rats, and RNi rats. Normobaric hypoxia significantly reduced locomotion in RN rats but not in RT rats. Both intraspecific and interspecific transcriptome analysis revealed that hypoxic exposure upregulated the expression of some genes related to hypoxic adaptation in RT rats but not in RN rats. The present study suggested that RT rats have unique genetic and phenotypic adaptations to hypoxia.

Genes specific to RT and shared with MM that are adapted to hypoxia

According to our comparative genomic analysis, RT rats might adapt to hypoxia for two reasons, but neither RN nor RR rats adapt to hypoxia. One piece of evidence was that, among the enrichment results for PSGs in the four lineages, only RT rats had terms related to hypoxia adaptation. In particular, members of the hypoxia-inducible factor (HIF) family, *Hif-2/3α*, were positively selected for in RT rats. *Hifs* are master regulators of the cellular response to hypoxia (Bigham & Lee 2014). Among these genes, *Epas1* (*Hif-2α*), involved in the regulation of erythropoietin transcription, is widely recognized as a candidate gene for adaptation to hypoxia in

other high-altitude species. *Epas1* has also undergone positive selection in Tibetan sheep, Tibetan gray wolves, and Tibetan individuals (Hu *et al.* 2019; Pamenter *et al.* 2020). *Hif-3α* inhibits the action of *Hif-1/2α* and activates a different transcriptional response to hypoxia (Zhang *et al.* 2014). Vascular development and erythropoiesis are adaptive changes that occur in low-altitude organisms at high altitudes (Simonson 2015; Hollerer *et al.* 2017). In RT rats, genes involved in angiogenesis (*Vegfa, Notch1, Mcam, Pdgfa, Ramp2*, and *Angpt2*) (Albertin *et al.* 2010; Krock *et al.* 2011; Palomero *et al.* 2014; Shao *et al.* 2015; Cai *et al.* 2020) and genes involved in erythropoiesis (*Hmox1* and *Slc29a1*) (Loboda *et al.* 2008; Zwifelhofer *et al.* 2020) were subjected to positive selection, which might result in these two functions being stronger in RT rats than in other species. Similarly, compared with lowland rodents, *Mcam* has undergone positive selection on plateau zokors (Shao *et al.* 2015). *Slc29a1* is a candidate gene for adapting to hypoxia in plateau zokors and the naked mole-rat (Pamenter *et al.* 2020).

Another piece of evidence was that RT and MM, rodents that have adapted to hypoxic environments, have undergone parallel evolution to adapt to hypoxia. Among the three *Rattus* species, only RT shared eight hypoxia-related REGs (*Adam9, Egln3, Arnt, Ednrb, Pgf, Sec24b, Pdgfa*, and *Angpt2*) with MM. In particular, *Adam9*, an important regulator of *Hif1-α*, which in turn regulates more than 100 hypoxia-inducible genes, is also under positive selection in ground tit and Tibetan human populations (Qu *et al.* 2013). *Egln3* regulates the stability of *Hif-1α* (Kelly *et al.* 2020). *Sirt2*, which belongs to MM, is also involved in mediating the stability of *Hif-1α* (Kaitsuka *et al.* 2021). *Arnt* (*Hif-1β*) plays a pivotal role in adaptive responses to hypoxia. It forms heterodimeric complexes with *Hif-1/2α*, activating hypoxia-inducible genes critical for angiogenesis, anaerobic metabolism, and other processes in response to O_2 deprivation (Imamura *et al.* 2014). *Ednrb, Pgf, Sec24b, Pdgfa,* and *Angpt2* are involved in blood vessel development (Bigham *et al.* 2010; Shao *et al.* 2015; Chédeville *et al.* 2020). *Spint1*, a REG of MM, is also related to angiogenesis (Shao *et al.* 2015).

It has been proposed that the successful colonization of MM in high-altitude environments is due to its origin in the Himalayan region, which gave MM preadaptation to low oxygen (Jochmans-Lemoine *et al.* 2016). However, genes associated with hypoxic adaptation in RT rats living at low altitudes that have not experienced hypoxic environments have been selected or are in a state of rapid evolution. Therefore, we suspected that RT rats might originate at high altitudes in India and Southeast Asia (Aplin *et al.* 2011).

Compared with those of related species, the energy metabolism and oxygen transport genes of RT have evolved

We next calculated the LD between polymorphic sites for all autosome regions in each species. Consistent with the findings of previous studies, we found that the LD decreased more rapidly in RT, RA, RL, and RNi populations than in the RN population, which was consistent with the lower levels of nucleotide diversity observed in the RN rats (Teng *et al.* 2017). Among the five *Rattus* species, RT exhibited the highest genetic diversity, which might be one of the reasons for the rapid expansion of its distribution range.

Compared with that in other *Rattus* species, the abundance of PSGs related to energy metabolism in the RT genome might facilitate adaptation to hypoxia. Hypoxic environments lead to reduced energy production through aerobic metabolism due to limited oxygen availability. Hence, glycolysis plays a crucial role in balancing energy supply and demand. As an illustration, glycolysis sustains the energy supply in high-altitude Tibetan sheep (Wen *et al.* 2021). Genes associated with glycolysis are also under positive selection in Tibetan yaks and Tibetan individuals (Tian *et al.* 2017; O'Brien *et al.* 2020). Some genes related to pyruvate metabolism in the second phase of anaerobic metabolism were also identified to be under positive selection in Tibetan yaks and marine cetaceans (Tian *et al.* 2017). Maintaining a high rate of fatty acid oxidation is essential for sustaining metabolic heat production under plateau conditions (Liu *et al.* 2023). For example, deer mice living at high altitudes have a greater ability to oxidize fatty acids, although this is the opposite of the results in humans (Cheviron *et al.* 2012). These findings imply that RT rats might have an advantage in sustaining energy supply in hypoxic environments relative to the other four *Rattus* species. Retinoids play an important role in many physiological processes, especially in reproduction and embryonic development (Blomhoff & Blomhoff 2006). Compared to that of other *Rattus* species, the positive selection of genes associated with retinoid metabolic processes might facilitate the establishment of populations in hypoxic environments via RT.

Augmenting oxygen transport capacity can also maintain the energy supply under hypoxia. Two distinctive nonsynonymous substitutions in the *Hbb* of the RT population, when compared to those of other *Rattus* species, could impact oxygen-transport capacity. HBB is a component of hemoglobin that is responsible for transporting O_2 from the lung to metabolizing tissues. It comprises

two α-chain (HBA) subunits and two β-chain (HBB) subunits (Storz & Moriyama 2008). Substituting amino acid residues on the subunit contact surface of hemoglobin (Hb) can alter the affinity of Hb-O_2. For example, a single amino acid point mutation, Pro199Ala, in HBA increases the Hb-O_2 affinity of the bar-headed goose (*Anser indicus*) compared to the graylag goose (*A. anser*) (Jessen *et al.* 1991; Weber *et al.* 1993). The substitution Leu55Ser in the HBB of Andean geese (*Chloephaga melanoptera*) results in a much greater affinity for Hb-O_2 than that in lowland mallard ducks (*Anas platyrhynchos*) (Jessen *et al.* 1991; Weber *et al.* 1993). The individual or combined effects of eight amino acid mutations in the HBB of high-altitude deer mice result in higher Hb-O_2 affinity than that of lowland deer mice (Storz *et al.* 2009). Two substitutions, Arg31Ser and Leu33Met, located on the subunit contact surface of HBB, were predicted by PolyPhen-2 to significantly alter HBB function, potentially resulting in markedly greater Hb-O_2 affinity and, consequently, enhanced oxygen transport capacity in RT rats than in other rat species. The positive selection of genes related to terpene metabolism may also increase the oxygen transport capacity of RT. For example, squalene is a triterpene produced by rats themselves and can carry oxygen independently of red blood cells. A variety of plant-derived terpenes can also promote blood circulation in animals (Güneş 2013; Powder-George 2024). Furthermore, additional PSGs within the RT versus RN group could impact oxygen-transport capacity. For instance, *Slc39a12* regulates hypoxia-induced pulmonary vascular remodeling, and *Ank2* and *Nos1ap* are involved in cardiac muscle or heart contraction (Cunha *et al.* 2008; Beech *et al.* 2010; Zhao *et al.* 2015).

Population genomic analysis revealed genetic traits in RT rats that might sustain energy supply in hypoxic environments, as demonstrated by the behavioral responses of RT and RN rats to hypoxia. In reality, many mammals react to hypoxia by decreasing activity, energy expenditure, and oxygen consumption. However, this strategy is not suitable for coping with reduced oxygen availability during aerobic exercise (Storz *et al.* 2010). RN rats might struggle to sustain their energy supply in a low-oxygen environment, causing them to reduce their activity and increase their rest time. The RT activity did not change, possibly due to the positive selection of genes linked to glycolysis and oxygen transport capacity in the RT genome, enabling them to uphold energy supply in hypoxic environments. In addition, we did not observe aggressive interactions between RT rats and RN rats caged together under either normoxic or hypoxic conditions, implying that the influence of interspecific interference competition on geographical distribution was less than the difference in hypoxic tolerance between RN and RT rats (Guo *et al.* 2017).

More hypoxia-related DEGs were detected in RT rats than in RN rats after normobaric hypoxia treatment

Under chronic hypoxic treatment, RT rats had a greater number of DEGs than RN rats did, consistent with previous findings in acute hypoxia (Chen *et al.* 2021a). Directly exposed to the atmosphere, the lung is among the key organs involved in adaptive transcriptional changes in response to high altitudes (Qi *et al.* 2019). Hypoxia can trigger apoptosis and consequently impair pulmonary function and the effectiveness of O_2 delivery (Woik & Kroll 2015). In the lungs of RT rats, the majority of upregulated genes were linked to cell division, potentially mitigating damage to lung tissue resulting from apoptosis. Certain genes associated with angiogenesis might enhance oxygen transport within lung tissue, consequently minimizing lung damage caused by hypoxia. These findings align with the functions of DEGs observed in the lungs of yaks residing at high altitudes (Ge *et al.* 2021). Conversely, in RN rats, certain pulmonary genes associated with muscle contractions and the extracellular matrix were downregulated under hypoxia, suggesting potential impairment of lung function (Zhou *et al.* 2018).

The response of the liver to hypoxia is vital for the organism. Like in mice, RT rats experiencing hypoxia exhibited upregulated hepatic genes associated with oxygen transport (Baze *et al.* 2010). Specifically, the upregulation of *Hbb* and *Alas2*, which as specific erythrocyte markers, indicated the activation of extramedullary hematopoietic function in the livers of RT rats (Gao *et al.* 2016). This will increase the HB concentration in RT, which might increase O_2 delivery. The upregulated genes related to insulin secretion might further enhance O_2 delivery in RT rats. Insulin could activate mTORC1-mediated signaling, and mTORC1 is a crucial regulator of erythrocyte growth and proliferation (Knight *et al.* 2014). Insulin can also induce the expression of vascular endothelial growth factor (VEGF), which promotes angiogenesis (Carnesecchi *et al.* 2006). Hypoxia promotes the production of reactive oxygen species (ROS), which lead to oxidative damage to biomolecules, including DNA, lipids, and proteins, when present in excess (McGarry *et al.* 2018). The upregulated genes in response to oxidative stress in

the RT liver suggested that oxidative damage to the liver by ROS might be reduced in RT rats.

The transcriptional changes in sperm indicated that the sperm quality of RT rats increased after hypoxia. For example, the upregulation of genes associated with amino acid catabolism and organic acid synthesis suggests active energy metabolism in RT sperm (Menezes *et al.* 2019). Upregulation of *Tnp2* suggested a potential reduction in the rate of sperm malformation in RT rats exposed to hypoxic conditions (Savadi-Shiraz *et al.* 2015). The upregulation of genes related to kinesin might facilitate the spermatogenesis process in RT rats (Ma *et al.* 2017). Certain genes related to embryo development were upregulated in RT sperm. These genes are associated with the coagulation process and dorsal/ventral pattern formation, both of which are pivotal in embryonic development and might increase reproductive success (Bugge *et al.* 1996). The downregulation of *Ervfrd-1*, a crucial gene in placental formation (West *et al.* 2022), could lead to a decrease in reproductive success for RN rats in hypoxic environments.

The immune system and its functions are energetically costly physiological activities that may involve trade-offs with other physiological processes when resources are limited (Sheldon & Verhulst 1996). Genes related to immunity were uniformly downregulated in the livers, lungs, and sperm of RT rats exposed to hypoxia. This could be due to the suppression of immune responses to conserve energy for vital activities such as movement, reproduction, and survival. These findings suggest that immunosuppression could be a significant physiological adaptation in RT rats to cope with hypoxic environments (Meehan 1987).

Interspecific transcriptome analysis also provided insights into how RT rats adapt to hypoxia. Under normoxic conditions, DEGs in the lungs, liver, and sperm were associated with various functions in RT and RN rats. In a hypoxic environment, genes highly expressed in RT lungs were mostly related to cell division and the regulation of blood pressure, which might increase the adaptability to hypoxia. Hypoxia can cause an increase in pulmonary blood pressure (Gurney 2002), which can overburden the right ventricle of the heart and contribute to pathophysiological conditions (León-Velarde *et al.* 2010). The enrichment of the highly expressed hepatic genes in RT rats was mostly involved in metabolic functions, especially fatty acid metabolism for hypoxic adaptation (Ni *et al.* 2014). In contrast, RN rats did not exhibit any enrichment terms associated with improved adaptability to hypoxia according to the enrichment analysis.

In the hypoxic environment, the expression of certain genes in the liver and lung was significantly greater in RT rats than in RN rats. These genes were not present among the DEGs identified in the intraspecific transcriptome, providing further support for our hypothesis. Specifically, the elevated expression of *Ftmt* and *Upk1a* indicated that *Hif-1α* plays a role in modulating the hypoxic adaptation of RT rats but not RN rats. The induction of FTMT by HIF-1α could reduce hypoxia-induced damage to the liver (Wu *et al.* 2019). HIF-1α binds to the hypoxia response element in the promoter region of UPK1A, thereby promoting glycolysis in the liver and lungs of RT rats under hypoxic conditions (Song *et al.* 2020). Moreover, overexpression of *Gpbar1* in RT rats might mitigate hypoxia-induced mitochondrial dysfunction, apoptosis, and inflammation (Li *et al.* 2020). The high expression of *Nox3* in RT rats exposed to hypoxia might promote insulin-induced expression of VEGF, contributing to angiogenesis and oxygen delivery (Carnesecchi *et al.* 2006). Elevated expression of *Ghr1* might benefit the growth and oxygen regulation of RT rats under hypoxic conditions (Vikeså *et al.* 2017).

In conclusion, we provided genomic, behavioral, and transcriptomic evidence that RT rats preadapted to hypoxia compared to other *Rattus* species, enabling it to successfully expand from low altitudes to high altitudes with limited oxygen availability. We also provided a useful paradigm for predicting potential invaders in other species, an interesting topic in invasion biology. Moreover, we generated high-quality sequencing data for RL and RA rats within the *Rattus* genus, marking the first dataset of its kind. This dataset will facilitate future in-depth investigations into various *Rattus* species. In population genomic analysis, the number of samples may limit our ability to detect selection, which may affect our interpretation of RT adaptation to hypoxia, particularly at the level of gene or amino acid substitution. Future studies require large-scale parallel sampling to further investigate rodent preadaptation to hypoxia.

ACKNOWLEDGMENTS

This work was supported by grants from the Major Program of the National Natural Science Foundation of China (No. 32090022), the National Key R&D Program of China (No. 2022YFC2602500), the Science and Technology Planning Project of Guangdong (2021B1212110003), and the Beijing Natural Science Foundation (No. 5192015).

CONFLICT OF INTEREST STATEMENT

All authors have read and approved the final manuscript. We declare there is no conflict of interest.

DATA AVAILABILITY STATEMENT

The raw sequence data reported in this paper have been deposited in the Genome Sequence Archive in the National Genomics Data Center, China National Center for Bioinformation/Beijing Institute of Genomics, Chinese Academy of Sciences (GSA: CRA005347, GSA: CRA008884) and are publicly accessible at https://ngdc.cncb.ac.cn/gsa.

REFERENCES

Vikeså V, Nankervis L, Hevrøy E (2017). High dietary energy level stimulates growth hormone receptor and feed utilization in large Atlantic salmon (*Salmo salar* L.) under hypoxic conditions. *Aquaculture Nutrition* **23**, 1193–203.

Adzhubei I, Jordan DM, Sunyaev SR (2013). Predicting functional effect of human missense mutations using PolyPhen-2. *Current Protocols in Human Genetics* **7**, 7–20.

Albertin G, Sorato E, Oselladore B *et al*. (2010). Involvement of vascular endothelial growth factor signaling in CLR/RAMP1 and CLR/RAMP2-mediated pro-angiogenic effect of intermedin on human vascular endothelial cells. *International Journal of Molecular Medicine* **26**, 289–94.

Aplin KP, Suzuki H, Chinen AA *et al*. (2011). Multiple geographic origins of commensalism and complex dispersal history of black rats. *PLoS ONE* **6**, e26357.

Arias-Reyes C, Soliz J, Joseph V (2021). Mice and rats display different ventilatory, hematological, and metabolic features of acclimatization to hypoxia. *Frontiers in Physiology* **12**, 647822.

Baze MM, Schlauch K, Hayes JP (2010). Gene expression of the liver in response to chronic hypoxia. *Physiological Genomics* **41**, 275–88.

Beech RD, Lowthert L, Leffert JJ *et al*. (2010). Increased peripheral blood expression of electron transport chain genes in bipolar depression. *Bipolar Disorders* **12**, 813–24.

Bigham A, Bauchet M, Pinto D *et al*. (2010). Identifying signatures of natural selection in Tibetan and andean populations using dense genome scan data. *PLoS Genetics* **6**, e1001116.

Bigham AW, Lee FS (2014). Human high-altitude adaptation: forward genetics meets the HIF pathway. *Genes & Development* **28**, 2189–204.

Blackwell T, Ford AGP, Ciezarek AG *et al*. (2021). Newly discovered cichlid fish biodiversity threatened by hybridization with non-native species. *Molecular Ecology* **30**, 895–911.

Blomhoff R, Blomhoff HK (2006). Overview of retinoid metabolism and function. *Journal of Neurobiology* **66**, 606–30.

Bugge TH, Xiao Q, Kombrinck KW *et al*. (1996). Fatal embryonic bleeding events in mice lacking tissue factor, the cell-associated initiator of blood coagulation. *PNAS* **93**, 6258–63.

Cai W, Liu S, Liu Z *et al*. (2020). Downregulation of lung miR-203a-3p expression by high-altitude hypoxia enhances VEGF/Notch signaling. *Aging* **12**, 4247–67.

Carnesecchi S, Carpentier JL, Foti M, Szanto I (2006). Insulin-induced vascular endothelial growth factor expression is mediated by the NADPH oxidase NOX3. *Experimental Cell Research* **312**, 3413–24.

Chen C, Chen H, Zhang Y *et al*. (2020). TBtools: an integrative toolkit developed for interactive analyses of big biological data. *Molecular Plant* **13**, 1194–202.

Chen H, Patterson N, Reich D (2010). Population differentiation as a test for selective sweeps. *Genome Research* **20**, 393–402.

Chen IC, Hill JK, Ohlemüller R, Roy DB, Thomas CD (2011). Rapid range shifts of species associated with high levels of climate warming. *Science (New York, N.Y.)* **333**, 1024–26.

Chen Y, Hou G, Jing M *et al*. (2021a). Genomic analysis unveils mechanisms of northward invasion and signatures of plateau adaptation in the Asian house rat. *Molecular Ecology* **30**, 6596–610.

Chen Y, Zhao L, Teng H *et al*. (2021b). Population genomics reveal rapid genetic differentiation in a recently invasive population of *Rattus norvegicus*. *Frontiers in Zoology* **18**, 6.

Cheviron ZA, Bachman GC, Connaty AD, McClelland GB, Storz JF (2012). Regulatory changes contribute to the adaptive enhancement of thermogenic capacity in high-altitude deer mice. *PNAS* **109**, 8635–40.

Chédeville AL, Lourdusamy A, Monteiro AR, Hill R, Madureira PA (2020). Investigating glioblastoma response to hypoxia. *Biomedicines* **8**, 310.

Cunha SR, Le Scouarnec S, Schott JJ, Mohler PJ (2008). Exon organization and novel alternative splicing of the human *ANK2* gene: Implications for cardiac function

and human cardiac disease. *Journal of Molecular and Cellular Cardiology* **45**, 724–34.

Danecek P, Auton A, Abecasis G *et al*. (2011). The variant call format and VCFtools. *Bioinformatics (Oxford, England)* **27**, 2156–58.

Edgar RC (2004). MUSCLE: Multiple sequence alignment with high accuracy and high throughput. *Nucleic Acids Research* **32**, 1792–97.

Emms DM, Kelly S (2019). OrthoFinder: Phylogenetic orthology inference for comparative genomics. *Genome Biology* **20**, 238.

Feng Z, Cai G, Zheng C (1986). *The Mammals of Tibet*. Science Press, Beijing.

Gao JL, Shui YM, Jiang W *et al*. (2016). Hypoxia pathway and hypoxia-mediated extensive extramedullary hematopoiesis are involved in ursolic acid's antimetastatic effect in 4T1 tumor bearing mice. *Oncotarget* **7**, 71802–16.

Ge Q, Guo Y, Zheng W *et al*. (2021). Molecular mechanisms detected in yak lung tissue via transcriptome-wide analysis provide insights into adaptation to high altitudes. *Scientific Reports* **11**, 7786.

Guo HL, Teng HJ, Zhang JH, Zhang JX, Zhang YH (2017). Asian house rats may facilitate their invasive success through suppressing brown rats in chronic interaction. *Frontiers in Zoology* **14**, 20.

Guo S, Li G, Liu J *et al*. (2019). Dispersal route of the Asian house rat (*Rattus tanezumi*) on mainland China: Insights from microsatellite and mitochondrial DNA. *BMC Genetics* **20**, 11.

Gurney AM (2002). Multiple sites of oxygen sensing and their contributions to hypoxic pulmonary vasoconstriction. *Respiratory Physiology & Neurobiology* **132**, 43–53.

Güneş FE (2013). Medical use of squalene as a natural antioxidant. *Journal of Marmara University Institute of Health Sciences* **3**, 220–28.

Hollerer I, Bachmann A, Muckenthaler MU (2017). Pathophysiological consequences and benefits of HFE mutations: 20 years of research. *Haematologica* **102**, 809–17.

Hu XJ, Yang J, Xie XL *et al*. (2019). The genome landscape of Tibetan sheep reveals adaptive introgression from argali and the history of early human settlements on the Qinghai-Tibetan plateau. *Molecular Biology and Evolution* **36**, 283–303.

Huang W, Xia L, Yang Q, Feng Z (2008). Distribution pattern and zoogeographical division of mammals on the Qinghai-Tibet Plateau. *Acta Theriologica Sinica* **28**, 375–94.

Imamura Y, Tomita S, Imanishi M *et al*. (2014). HIF-2α/ARNT complex regulates hair development *via* induction of $p21^{Waf1/Cip1}$ and $p27^{Kip1}$. *FASEB Journal: Official Publication of the Federation of American Societies for Experimental Biology* **28**, 2517–24.

Indriastuti R, Pardede BP, Gunawan A *et al*. (2022). Sperm transcriptome analysis accurately reveals male fertility potential in livestock. *Animals* **12**, 2955.

Jessen TH, Weber RE, Fermi G, Tame J, Braunitzer G (1991). Adaptation of bird hemoglobins to high altitudes: demonstration of molecular mechanism by protein engineering. *PNAS* **88**, 6519–22.

Jing M, Chen Y, Yao K, Wang Y, Huang L (2022). Comparative phylogeography of two commensal rat species (*Rattus tanezumi* and *Rattus norvegicus*) in China: Insights from mitochondrial DNA, microsatellite, and 2b-RAD data. *Ecology and Evolution* **12**, e9409.

Jochmans-Lemoine A, Shahare M, Soliz J, Joseph V (2016). HIF1α and physiological responses to hypoxia are correlated in mice but not in rats. *Journal of Experimental Biology* **219**, 3952–61.

Jochmans-Lemoine A, Villalpando G, Gonzales M *et al*. (2015). Divergent physiological responses in laboratory rats and mice raised at high altitude. *Journal of Experimental Biology* **218**, 1035–43.

Kaitsuka T, Matsushita M, Matsushita N (2021). Regulation of hypoxic signaling and oxidative stress via the MicroRNA-SIRT2 axis and its relationship with aging-related diseases. *Cells* **10**, 3316.

Kelly T, Johnsen H, Burgerhout E *et al*. (2020). Low oxygen stress during early development influences regulation of hypoxia-response genes in farmed Atlantic salmon (*Salmo salar*). *G3 (Bethesda, Md.)* **10**, 3179–88.

Kim D, Langmead B, Salzberg SL (2015). HISAT: A fast spliced aligner with low memory requirements. *Nature Methods* **12**, 357–60.

Knight ZA, Schmidt SF, Birsoy K, Tan K, Friedman JM (2014). A critical role for mTORC1 in erythropoiesis and anemia. *eLife* **3**, e01913.

Kosoy M, Khlyap L, Cosson J-F, Morand S (2015). Aboriginal and invasive rats of genus *Rattus* as hosts of infectious agents. *Vector-Borne and Zoonotic Diseases* **15**, 3–12.

Krock BL, Skuli N, Simon MC (2011). Hypoxia-induced angiogenesis: Good and evil. *Genes & Cancer* **2**, 1117–33.

Lee TH, Guo H, Wang X, Kim C, Paterson AH (2014). SNPhylo: A pipeline to construct a phylogenetic tree from huge SNP data. *BMC Genomics* **15**, 162.

León-Velarde F, Villafuerte FC, Richalet J-P (2010). Chronic mountain sickness and the heart. *Progress in Cardiovascular Diseases* **52**, 540–49.

Li GC, Meng FX, Zhang G *et al*. (2009a). Investigation of distribution along the Qinghai?Tibet railway and other areas in Tibet autonomous region. *Chinese Journal of Vector Biology & Control* **20**, 213–15.

Li H, Durbin R (2009). Fast and accurate short read alignment with Burrows-Wheeler transform. *Bioinformatics (Oxford, England)* **25**, 1754–60.

Li H, Handsaker B, Wysoker A *et al*. (2009b). The Sequence Alignment/Map format and SAMtools. *Bioinformatics (Oxford, England)* **25**, 2078–79.

Li J, Cheng R, Wan H (2020). Overexpression of TGR5 alleviates myocardial ischemia/reperfusion injury via AKT/GSK-3β mediated inflammation and mitochondrial pathway. *Bioscience Reports* **40**, BSR20193482.

Liu G, Li Y, Liao N *et al*. (2023). Energy metabolic mechanisms for high altitude sickness: Downregulation of glycolysis and upregulation of the lactic acid/amino acid-pyruvate-TCA pathways and fatty acid oxidation. *Science of The Total Environment* **894**, 164998.

Liu Y, Yao L, Ci Y *et al*. (2021). Genetic differentiation of geographic populations of *Rattus tanezumi* based on the mitochondrial *Cytb* gene. *PLoS ONE* **16**, e0248102.

Loboda A, Jazwa A, Grochot-Przeczek A *et al*. (2008). Heme oxygenase-1 and the vascular bed: From molecular mechanisms to therapeutic opportunities. *Antioxidants & Redox Signaling* **10**, 1767–812.

Love MI, Huber W, Anders S (2014). Moderated estimation of fold change and dispersion for RNA-seq data with DESeq2. *Genome Biology* **15**, 550.

Ma DD, Wang DH, Yang WX (2017). Kinesins in spermatogenesis. *Biology of Reproduction* **96**, 267–76.

McGarry T, Biniecka M, Veale DJ, Fearon U (2018). Hypoxia, oxidative stress and inflammation. *Free Radical Biology & Medicine* **125**, 15–24.

McKenna A, Hanna M, Banks E *et al*. (2010). The genome analysis toolkit: A mapreduce framework for analyzing next-generation DNA sequencing data. *Genome Research* **20**, 1297–303.

Meehan RT (1987). Immune suppression at high altitude. *Annals of Emergency Medicine* **16**, 974–79.

Menezes EB, Velho ALC, Santos F *et al*. (2019). Uncovering sperm metabolome to discover biomarkers for bull fertility. *BMC Genomics* **20**, 714.

Ni Q, Shao Y, Wang YZ, Jing YH, Zhang YC (2014). Impact of high altitude on the hepatic fatty acid oxidation and synthesis in rats. *Biochemical and Biophysical Research Communications* **446**, 574–79.

O'Brien KA, Simonson TS, Murray AJ (2020). Metabolic adaptation to high altitude. *Current Opinion in Endocrine and Metabolic Research* **11**, 33–41.

Palomero J, Vegliante MC, Rodríguez ML *et al*. (2014). SOX11 promotes tumor angiogenesis through transcriptional regulation of PDGFA in mantle cell lymphoma. *Blood* **124**, 2235–47.

Pamenter ME, Hall JE, Tanabe Y, Simonson TS (2020). Cross-species insights into genomic adaptations to hypoxia. *Frontiers in Genetics* **11**, 743.

Pendleton AL, Shen F, Taravella AM *et al*. (2018). Comparison of village dog and wolf genomes highlights the role of the neural crest in dog domestication. *BMC Biology* **16**, 64.

Pertea M, Pertea GM, Antonescu CM *et al*. (2015). StringTie enables improved reconstruction of a transcriptome from RNA-seq reads. *Nature Biotechnology* **33**, 290–95.

Powder-George YL (2024). Chapter 10 - terpenoids. In the previous edition, A. Ludwiczuk, K. Skalicka-Woźniak, and M.I. Georgiev contributed to this chapter. In: McCreath SB, Clement YN, eds. *Pharmacognosy*, 2nd edn. Academic Press, Cambridge, MA, pp. 253–94.

Provan J, Maggs CA (2012). Unique genetic variation at a species' rear edge is under threat from global climate change. *Proceedings. Biological Sciences* **279**, 39–47.

Qi X, Zhang Q, He Y *et al*. (2019). The transcriptomic landscape of yaks reveals molecular pathways for high altitude adaptation. *Genome Biology and Evolution* **11**, 72–85.

Qiu Q, Zhang G, Ma T *et al*. (2012). The yak genome and adaptation to life at high altitude. *Nature Genetics* **44**, 946–49.

Qu Y, Zhao H, Han N *et al*. (2013). Ground tit genome reveals avian adaptation to living at high altitudes in the Tibetan plateau. *Nature Communications* **4**, 2071.

Rowe KC, Aplin KP, Baverstock PR, Moritz C (2011). Recent and rapid speciation with limited morphological disparity in the genus *Rattus*. *Systematic Biology* **60**, 188–203.

Sabeti PC, Varilly P, Fry B *et al*. (2007). Genome-wide detection and characterization of positive selection in human populations. *Nature* **449**, 913–18.

Savadi-Shiraz E, Edalatkhah H, Talebi S *et al*. (2015). Quantification of sperm specific mRNA transcripts (*PRM1*, *PRM2*, and *TNP2*) in teratozoospermia and normozoospermia: New correlations between mRNA content and morphology of sperm. *Molecular Reproduction and Development* **82**, 26–35.

Shakya M, Ahmed SA, Davenport KW *et al*. (2020). Standardized phylogenetic and molecular evolutionary analysis applied to species across the microbial tree of life. *Scientific Reports* **10**, 1723.

Shao Y, Li JX, Ge RL *et al*. (2015). Genetic adaptations of the plateau zokor in high-elevation burrows. *Scientific Reports* **5**, 17262.

Sheldon BC, Verhulst S (1996). Ecological immunology: Costly parasite defences and trade-offs in evolutionary ecology. *Trends in Ecology & Evolution* **11**, 317–21.

Simonson TS (2015). Altitude adaptation: A glimpse through various lenses. *High Altitude Medicine & Biology* **16**, 125–37.

Song Y, Wang H, Zou XJ *et al*. (2020). Reciprocal regulation of HIF-1α and Uroplakin 1A promotes glycolysis and proliferation in hepatocellular carcinoma. *Journal of Cancer* **11**, 6737–47.

Storz JF, Moriyama H (2008). Mechanisms of hemoglobin adaptation to high altitude hypoxia. *High Altitude Medicine & Biology* **9**, 148–57.

Storz JF, Runck AM, Sabatino SJ *et al*. (2009). Evolutionary and functional insights into the mechanism underlying high-altitude adaptation of deer mouse hemoglobin. *PNAS* **106**, 14450–55.

Storz JF, Scott GR, Cheviron ZA (2010). Phenotypic plasticity and genetic adaptation to high-altitude hypoxia in vertebrates. *Journal of Experimental Biology* **213**, 4125–36.

Szpiech ZA, Hernandez RD (2014). selscan: An efficient multithreaded program to perform EHH-based scans for positive selection. *Molecular Biology and Evolution* **31**, 2824–27.

Teng H, Zhang Y, Shi C *et al*. (2017). Population genomics reveals speciation and introgression between brown Norway rats and their sibling species. *Molecular Biology and Evolution* **34**, 2214–28.

Tian R, Yin D, Liu Y *et al*. (2017). Adaptive evolution of energy metabolism-related genes in hypoxia-tolerant mammals. *Frontiers in Genetics* **8**, 205.

Weber RE, Jessen TH, Malte H, Tame J (1993). Mutant hemoglobins (alpha 119-Ala and beta 55-Ser): Functions related to high-altitude respiration in geese. *Journal of Applied Physiology* **75**, 2646–55.

Wen Y, Hu J, Wang J *et al*. (2021). Effect of glycolysis and heat shock proteins on hypoxia adaptation of Tibetan sheep at different altitude. *Gene* **803**, 145893.

West RC, Ezashi T, B Schoolcraft W, Yuan Y (2022). Beyond fusion: A novel role for ERVW-1 in trophoblast proliferation and type I interferon receptor expression. *Placenta* **126**, 150–59.

Wilson DE, Reeder DM (2005). *Mammal Species of the World: A Taxonomic and Geographic Reference*, vol. 1. JHU Press, Baltimore, MD.

Woik N, Kroll J (2015). Regulation of lung development and regeneration by the vascular system. *Cellular and Molecular Life Sciences: CMLS* **72**, 2709–18.

Wu Q, Wu WS, Su L *et al*. (2019). Mitochondrial ferritin is a hypoxia-inducible factor 1α-inducible gene that protects from hypoxia-induced cell death in brain. *Antioxidants & Redox Signaling* **30**, 198–212.

Wu T, Hu E, Xu S *et al*. (2021). clusterProfiler 4.0: A universal enrichment tool for interpreting omics data. *The Innovation* **2**, 100141.

Yang J, Lee SH, Goddard ME, Visscher PM (2011). GCTA: A tool for genome-wide complex trait analysis. *American Journal of Human Genetics* **88**, 76–82.

Yang Z (2007). PAML 4: Phylogenetic analysis by maximum likelihood. *Molecular Biology and Evolution* **24**, 1586–91.

Zhang C, Dong SS, Xu JY, He WM, Yang TL (2019). PopLDdecay: A fast and effective tool for linkage disequilibrium decay analysis based on variant call format files. *Bioinformatics (Oxford, England)* **35**, 1786–88.

Zhang MW, Guo C, Wang Y, Hu ZJ, Chen AG (2000). The buff-breasted rats (*Rattus flavipectus*) in China. *Zoological Research* **21**, 487–97.

Zhang P, Yao Q, Lu L *et al*. (2014). Hypoxia-inducible factor 3 is an oxygen-dependent transcription activator and regulates a distinct transcriptional response to hypoxia. *Cell Reports* **6**, 1110–21.

Zhao L, Oliver E, Maratou K *et al*. (2015). The zinc transporter ZIP12 regulates the pulmonary vascular response to chronic hypoxia. *Nature* **524**, 356–60.

Zhou Y, Horowitz JC, Naba A *et al*. (2018). Extracellular matrix in lung development, homeostasis and disease. *Matrix Biology* **73**, 77–104.

Zhou Y, Zhou B, Pache L *et al*. (2019). Metascape provides a biologist-oriented resource for the analysis of systems-level datasets. *Nature Communications* **10**, 1523.

Zwifelhofer NM, Cai X, Liao R *et al*. (2020). GATA factor-regulated solute carrier ensemble reveals a nucleoside transporter-dependent differentiation mechanism. *PLoS Genetics* **16**, e1009286.

SUPPLEMENTARY MATERIALS

Additional supporting information may be found online in the Supporting Information section at the end of the article.

Figure S1 Enrichment result of the shared positive selection genes of RT versus (vs) other rat species.

Figure S2 The common enrichment terms of RT vs other rat species.

Figure S3 Amino acid substitution scores of HBB in R. tanezumi were predicted using PolyPhen-2.

Figure S4 Lung transcriptome results from principal component analysis and heat map.

Figure S5 Hepatic transcriptome results from principal component analysis and heat map.

Figure S6 Sperm transcriptome results from principal component analysis and heat map.

Figure S7 Number of DEGs of intraspecific transcriptome analysis in liver, lung, and sperm of RT and RN after hypoxia.

Figure S8 Enrichment results of high expression genes in the lungs of RTs at interspecies transcriptome under normoxic conditions.

Figure S9 Enrichment results of high expression genes in the lungs of RNs at interspecies transcriptome under normoxic conditions.

Figure S10 Enrichment results of high expression genes in the livers of RTs at interspecies transcriptome under normoxic conditions.

Figure S11 Enrichment results of high expression genes in the livers of RNs at interspecies transcriptome under normoxic conditions.

Figure S12 Enrichment results of high expression genes in the sperm of RTs at interspecies transcriptome under normoxic conditions.

Figure S13 Enrichment results of high expression genes in the sperm of RNs at interspecies transcriptome under normoxic conditions.

Figure S14 Normalized gene-count heatmaps for genes associated with hypoxic adaptation in RT.

Figure S15 Quantitative RT-PCR results show the mRNA expression level of 10 genes in RT.

Table S1 Genome assemblies analyzed for compartive genome analyses.

Table S2 Whole genome sequenceing for population genome analysis.

Table S3 Selected genes and primers used for qRT-PCR.

Table S4 CT values of qRT-PCR.

Table S5 Positive selection genes calculated from the foreground clade of RN.

Table S6 Positive selection genes calculated from the foreground clade of RR.

Table S7 Positive selection genes calculated from the foreground clade of RT.

Table S8 Positive selection genes calculated from the foreground clade of *Mus musculus*.

Table S9 Rapidly evolving genes calculated from the foreground clade of RN.

Table S10 Rapidly evolving genes calculated from the foreground clade of RR.

Table S11 Rapidly evolving genes calculated from the foreground clade of RT.

Table S12 Rapidly evolving genes calculated from the foreground clade of *Mus musculus*.

Table S13 Positive selection genes of RT-RL.

Table S14 Positive selection genes of RT-RA.

Table S15 Positive selection genes of RT-RNi.

Table S16 Positive selection genes of RT-RN.

Cite this article as:

Cao R, Zhang M, Chen Y *et al.* (2024). The special adaptation to hypoxia facilitated the expansion of the Asian house rat (*Rattus tanezumi*) into Tibet but not other *Rattus* species. *Integrative Zoology* **00,** 1–18. https://doi.org/10.1111/1749-4877.12829